

Relationship between the Electron Density of the Heme Fe Atom and the Vibrational Frequencies of the Fe-Bound Carbon Monoxide in Myoglobin

Ryu Nishimura,[†] Tomokazu Shibata,[†] Hulin Tai,[†] Izumi Ishigami,[‡] Takashi Ogura,^{*,‡} Satoshi Nagao,[§] Takashi Matsuo,[§] Shun Hirota,[§] Kiyohiro Imai,^{||} Saburo Neya,[⊥] Akihiro Suzuki,[#] and Yasuhiko Yamamoto^{*,†}

[†]Department of Chemistry, University of Tsukuba, Tsukuba 305-8571, Japan

[‡]Department of Life Science, Graduate School of Life Science, University of Hyogo, Kamigori-cho, Ako-gun, Hyogo 678-1297, Japan

[§]Graduate School of Materials Science, Nara Institute of Science and Technology, Ikoma, Nara 630-0192, Japan

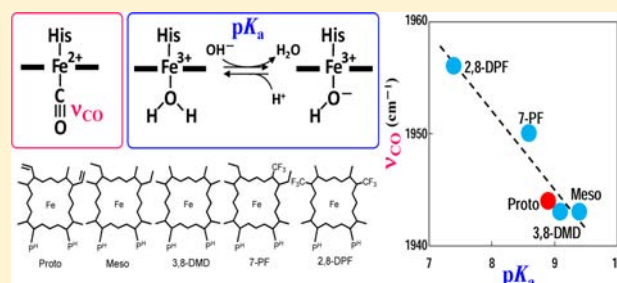
^{||}Department of Frontier Bioscience, Faculty of Bioscience and Applied Chemistry, Hosei University, Koganei, Tokyo 184-8584, Japan

[⊥]Department of Physical Chemistry, Graduate School of Pharmaceutical Sciences, Chiba University, Chuoh-Inohana, Chiba 260-8675, Japan

[#]Department of Materials Engineering, Nagaoka National College of Technology, Nagaoka 940-8532, Japan

Supporting Information

ABSTRACT: We analyzed the vibrational frequencies of the Fe-bound carbon monoxide (CO) of myoglobin reconstituted with a series of chemically modified heme cofactors possessing a heme Fe atom with a variety of electron densities. The study revealed that the stretching frequency of Fe-bound CO (ν_{CO}) increases with decreasing electron density of the heme Fe atom (ρ_{Fe}). This finding demonstrated that the ν_{CO} value can be used as a sensitive measure of the ρ_{Fe} value and that the π back-donation of the heme Fe atom to CO is affected by the heme π -system perturbation induced through peripheral side chain modifications.



INTRODUCTION

Myoglobin (Mb), the oxygen (O_2) storage hemoprotein, has served as a useful model system for delineating the structure–function relationships of proteins.^{1–6} O_2 binds reversibly to the ferrous heme Fe atom in Mb, and the O_2 binding properties of the protein have been shown to be obtained through subtle tuning of the intrinsic heme Fe reactivity in addition to the heme environment furnished by nearby amino acid residues.^{4,5} The importance of the heme electronic structure, particularly the electron density of the heme Fe atom (ρ_{Fe}), in the regulation of the heme Fe reactivity in the protein is now beginning to be realized.^{7,8} Hence, establishment of a methodology for quantitative estimation of the ρ_{Fe} value of Mb is needed to gain a deeper understanding of the molecular mechanism responsible for regulation of the heme Fe reactivity through the ρ_{Fe} value. We previously used the equilibrium constant, $\text{p}K_{\text{a}}$, of the so-called “acid–alkaline transition” in metmyoglobin (metMb) to estimate the ρ_{Fe} value of the protein (see Figure S1, Supporting Information).⁷ MetMb possessing highly conserved distal His64 has H_2O and OH^- as coordinated external ligands under low- and high-pH conditions, respectively.^{3,9–12} The ρ_{Fe} value is manifested in the $\text{p}K_{\text{a}}$ one through its effect on the H^+ affinity of the Fe^{3+} -

bound OH^- . Thus, this methodology is applicable only to Mbs capable of accommodating H_2O as an external ligand to the ferric heme Fe atom under low pH conditions. Generally, in Mbs lacking distal His64, irrespective of whether they are naturally occurring mutants^{13–18} or genetic ones,¹⁹ the sixth coordination site is either partially occupied by H_2O or empty. Consequently, other physicochemical parameters are needed to estimate the ρ_{Fe} values of the proteins.

In this study, we focused on carbon monoxide (CO) adducts of Mbs (MbCOs) because not only CO is known to be inevitably bound to the proteins but also the proteins each possess a physiologically active ferrous heme Fe atom. We observed the vibrational frequencies of the Fe-bound CO,^{20–22} that is, the stretching frequency of Fe-bound CO (ν_{CO}) and the Fe–C stretching (ν_{FeC}) and Fe–C–O bending frequencies (δ_{FeCO}) in native Mb and proteins reconstituted with mesoheme (Meso), 3,8-dimethyldeuteroporphyrinatoiron(III)^{23,24} (3,8-DMD), 13,17-bis(2-carboxylatoethyl)-3,8-diethyl-2,12,18-trimethyl-7-trifluoromethylporphyrinatoiron(III)²⁵ (7-PF), and 13,17-bis(2-carboxylatoethyl)-3,7-diethyl-12,18-

Received: December 26, 2012

Published: February 27, 2013

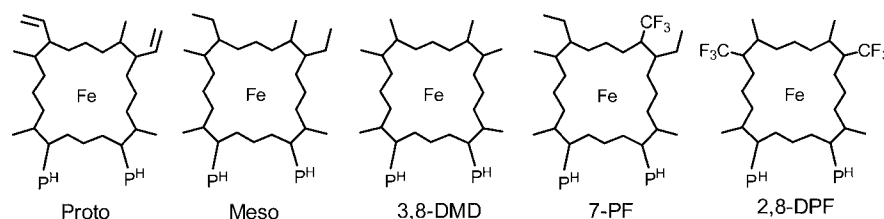


Figure 1. Schematic representation of the structures of the heme cofactors used in this study, that is, protoheme (Proto), mesoheme (Meso), 3,8-dimethyldeuterioporphyrinatoiron(III)^{23,24} (3,8-DMD), 13,17-bis(2-carboxylatoethyl)-3,8-diethyl-2,12,18-trimethyl-7-trifluoromethylporphyrinatoiron(III)²⁵ (7-PF), and 13,17-bis(2-carboxylatoethyl)-3,7-diethyl-12,18-trimethyl-2,8-difluoromethylporphyrinatoiron(III)⁷ (2,8-DPF). Abbreviation: P^H represents $-\text{CH}_2\text{CH}_2\text{COOH}$.

Table 1. O₂ and CO Binding Parameters and Autoxidation Reaction Rates for Mbs

Mb	O ₂ binding				k_{ox}^d (h ⁻¹) ^b	CO binding				M^f
	$k_{\text{on}}(\text{O}_2)^a$ ($\mu\text{M}^{-1}\text{s}^{-1}$)	$k_{\text{off}}(\text{O}_2)^a$ (s ⁻¹)	$K(\text{O}_2)^b$ (μM^{-1})	P_{50}^c (mmHg)		$k_{\text{on}}(\text{CO})^a$ ($\mu\text{M}^{-1}\text{s}^{-1}$)	$k_{\text{off}}(\text{CO})^a$ (s ⁻¹)	$K(\text{CO})^e$ (μM^{-1})		
Mb(Meso) ^g	8.2 ± 1.6	5.7 ± 1.1	1.4 ± 0.4	0.38	0.16 ± 0.02	0.38 ± 0.07	0.048 ± 0.009	7.9 ± 2.4	5.5 ± 2.2	
Mb(3,8-DMD)	12 ± 3	9.4 ± 3	1.3 ± 0.2	0.50	0.14 ± 0.01	0.16 ± 0.07	0.024 ± 0.007	6.7 ± 1.7	5.2 ± 2.1	
Native Mb ^h	14 ± 3	12 ± 2	1.2 ± 0.3	0.58	0.051 ± 0.005	0.51 ± 0.06	0.019 ± 0.005	27 ± 8	23 ± 9	
Mb(7-PF) ^g	8.3 ± 1.6	17 ± 3	0.5 ± 0.1	1.10	0.033 ± 0.003	0.32 ± 0.06	0.032 ± 0.006	10 ± 3	21 ± 8	
jMb(2,8-DPF) ^g	16 ± 3	110 ± 22	0.15 ± 0.04	2.80	0.083 ± 0.008	0.69 ± 0.13	0.036 ± 0.007	19 ± 6	132 ± 53	

^aMeasured at pH 7.40 and 25 °C. ^bCalculated from the $k_{\text{on}}(\text{O}_2)$ and $k_{\text{off}}(\text{O}_2)$ values. ^cDetermined from the oxygen equilibrium curve at pH 7.40 and 20 °C. ^dAutoxidation reaction rates measured at pH 7.40 and 35 °C. ^eCalculated from the $k_{\text{on}}(\text{CO})$ and $k_{\text{off}}(\text{CO})$ values. ^f $M = K(\text{CO})/K(\text{O}_2)$. ^gObtained from ref 7. ^hObtained from ref 30.

trimethyl-2,8-difluoromethylporphyrinatoiron(III)⁷ (2,8-DPF), that is, Mb(Meso), Mb(3,8-DMD), Mb(7-PF), and Mb(2,8-DPF), respectively. These heme cofactors differ in the numbers of CF₃, CH₃, and C₂H₅ side chains (Figure 1). On the basis of the pK_a values of the proteins, these heme cofactors could be ranked as Mb(2,8-DPF) < Mb(7-PF) < Mb(3,8-DMD) ≈ Mb(Meso) in order of increasing ρ_{Fe} value (see Figure S1, Supporting Information).⁷ We found that the ν_{CO} value of a protein correlates well with the pK_a value in such a manner that Mb possessing a lower pK_a value exhibits a higher ν_{CO} one. The relationship between the ν_{CO} and the pK_a (and hence ρ_{Fe}) values could be interpreted in terms of the resonance between the two canonical forms of the Fe–CO fragment (see below).²⁶ The study not only revealed the relationship between the ν_{CO} and the ρ_{Fe} values but also demonstrated that the ν_{CO} value can be used as a sensitive measure of the ρ_{Fe} one in the protein.

MATERIALS AND METHODS

Materials and Protein Samples. All reagents and chemicals were obtained from commercial sources and used as received. Sperm whale Mb was purchased as a lyophilized powder from Biozyme and used without further purification. Mesoheme (Meso) was purchased from Frontier Scientific Co. 3,8-DMD,^{23,24} 7-PF,²⁵ and 2,8-DPF⁷ were synthesized as previously described. The apoprotein of Mb (apoMb) was prepared at 4 °C according to the procedure of Teale²⁷ and reconstituted Mbs were prepared by slow addition of a synthetic heme cofactor to the apoMb in 50 mM potassium phosphate buffer, pH 7.0, at 4 °C.⁷ In order to prepare MbCO, metMb was reduced by adding Na₂S₂O₄ (Nakalai Chemicals Ltd.) in the presence of CO gas (Japan Air Gases), and then the protein was freed from excess reagents by passage through a Sephadex G-10 (Sigma-Aldrich Co.) column equilibrated with an appropriate buffer solution. The met-cyano form of the protein was prepared by addition of potassium cyanide (Sigma-Aldrich Co.) to metMb. The pH of each sample was measured with a Horiba F-22 pH meter equipped with a Horiba type 6069-10c electrode. The pH of a sample was adjusted using 0.1 M NaOH or HCl.

Kinetic Measurements of O₂ and CO Binding of Mb(3,8-DMD). Kinetic measurements of O₂ and CO binding of Mb(3,8-DMD) were carried out in 100 mM phosphate buffer, pH 7.40, at 20 °C, as described previously.^{3,28–31} The rate constant for O₂ association ($k_{\text{on}}(\text{O}_2)$) for the protein was determined through analysis of the time evolution of the absorbance at 425 nm after photolysis of the oxy form in the presence of various O₂ concentrations using a 5 ns pulse Nd:YAG laser (532 nm). The pseudo-first-order rate constant for O₂ dissociation ($k_{\text{off}}(\text{O}_2)$) for the protein was also measured through analysis of the time evolution of the absorbance at 425 nm after rapidly mixing the oxy form with excess Na₂S₂O₄ using a stopped-flow apparatus (Unisoku, Co. Ltd., Osaka, Japan). The equilibrium constants for O₂ binding ($K(\text{O}_2)$) were calculated from the kinetic data, that is, the $k_{\text{on}}(\text{O}_2)$ and $k_{\text{off}}(\text{O}_2)$ values.

The rate constant for CO association ($k_{\text{on}}(\text{CO})$) of the protein was similarly measured through analysis of the time evolution of the absorbance at 407 nm after photolysis of the CO form under 1 atm of CO, that is, the concentration of CO ([CO]) = 9.85 × 10⁻⁴ M. The $k_{\text{on}}(\text{CO})$ value can be determined from the observed pseudo-first-order rate constant for CO association ($k_{\text{obs}}(\text{CO})$) using the equation $k_{\text{obs}}(\text{CO}) \approx k_{\text{on}}(\text{CO})$ because the rate constant of the CO dissociation ($k_{\text{off}}(\text{CO})$) is $\ll k_{\text{on}}(\text{CO}) \times [\text{CO}]$. Then, the $k_{\text{off}}(\text{CO})$ value was determined by analysis of displacement of Fe-bound CO and oxidation of heme Fe by K₃Fe(CN)₆.^{28,29,31} Similar to the case of the study of O₂ binding, the equilibrium constants for CO binding ($K(\text{CO})$) were calculated from the kinetic data, that is, the $k_{\text{on}}(\text{CO})$ and $k_{\text{off}}(\text{CO})$ values.

Resonance Raman Spectroscopy. Resonance Raman scattering was performed with excitation at 413.1 nm with a Kr⁺ laser (Spectra Physics, BeamLok 2060), dispersed with a polychromator (SPEX 1877, 1200 grooves/mm grating) and detected with a liquid-nitrogen-cooled charge-coupled device (CCD) detector (CCD-1024 × 256-OPEN-1LS, HORIBA Jobin Yvon).³² A laser power of 1.6 mW was used for the measurements. CO isotopes, that is, ¹³C¹⁶O and ¹³C¹⁸O, were purchased from SI Science Co., Ltd., Japan. Raman shifts were calibrated with indene as a frequency standard. The accuracy of the peak positions of well-defined Raman bands was ±1 cm⁻¹. Protein concentrations were approximately 40 μM in 100 mM potassium phosphate buffer, pH 7.4.

RESULTS

Functional Consequences of Heme Modifications. We measured the O₂ and CO binding kinetics of Mb(3,8-DMD) (see Figure S2, Supporting Information), and the results are compared with those for other proteins reported previously⁷ (Table 1). The O₂ affinities of the proteins were also compared with each other on the basis of the *P*₅₀ value, which is the partial pressure of O₂ required to achieve 50% oxygenation (Table 1). Since 7-PF and 2,8-DPF can be considered as counterparts of Meso and 3,8-DMD, respectively, the effects of the substitution of one and two CF₃ groups on the kinetic data could be inferred from the results of comparative studies on Mb(Meso) and Mb(7-PF), and Mb(3,8-DMD) and Mb(2,8-DPF), respectively. In the case of O₂ binding, the *k*_{on}(O₂) value of a protein was essentially independent of the number of CF₃ substitution(s), while the *k*_{off}(O₂) one increased by a factor of ~3 upon introduction of one CF₃ group. As a result, the O₂ affinity of the protein decreased with increasing number of CF₃ substitutions, as demonstrated previously.⁷ On the other hand, the effects of CF₃ substitution(s) on the *k*_{on}(CO) and *k*_{off}(CO) values varied with the system. Both the *k*_{on}(CO) and the *k*_{off}(CO) values slightly decreased on substitution of one CF₃ group, as demonstrated for the Mb(Meso)/Mb(7-PF) system and, in contrast, increased on substitution of two CF₃ ones, as revealed through analysis of the Mb(3,8-DMD)/Mb(2,8-DPF) system. In addition, the CO affinity of the protein was essentially unaltered by substitution of one CF₃ group but increased by a factor of ~2.8 on substitution of two CF₃ ones. The apparent lack of consistency in the effect of the number of the CF₃ substitution(s) on the *k*_{on}(CO) and *k*_{off}(CO) values would be due to the presence of a significant “heme orientational disorder”³³ in Mb(7-PF) (see below).

The ability of Mb to stabilize Fe-bound O₂ and discriminate against CO binding can be evaluated on the basis of the ratio of CO to O₂ affinity, that is, the *K*(CO)/*K*(O₂) value, which is usually represented by the *M* value.³⁴ *M* values of the proteins demonstrated remarkable effects of the ρ_{Fe} value on the discrimination between O₂ and CO (Table 1), as reported previously.⁷ The *M* value increased by a factor of ~4 on substitution of one CF₃ group, as demonstrated for the Mb(Meso)/Mb(7-PF) system, and then by a factor of ~25 on substitution of two CF₃ ones, as revealed through analysis of the Mb(3,8-DMD)/Mb(2,8-DPF) system. These results demonstrated that the heme electronic structure plays a significant role in the discrimination of exogenous ligands by the protein.

Vibrational Frequencies of Fe-Bound CO. We determined the ν_{CO} , ν_{FeC} and δ_{FeCO} values of native MbCO, MbCO(Meso), MbCO(3,8-DMD), MbCO(7-PF), and MbCO(2,8-DPF). The ν_{CO} band of the protein contained multiple components (Figure 2 and Figures S3–S7, Supporting Information), and the observation of multiple ν_{CO} bands is not due to the heme orientational disorder, because of the observation of similar multiple bands in the spectra of Mbs reconstituted with C₂-symmetric hemes, that is, 3,8-DMD and 2,8-DPF. We also exclude the possibility of Fermi resonance, which is observed in the case of incidental frequency overlap between two oscillators, that is, CO- and Fe-bound histidyl imidazole ring. The doublets in Figure 2 are not interpreted as a consequence of Fermi resonance, since the doublets are evident for the five species. Consequently, the doublets in Figure 2 are due to the presence of multiple conformational states of the

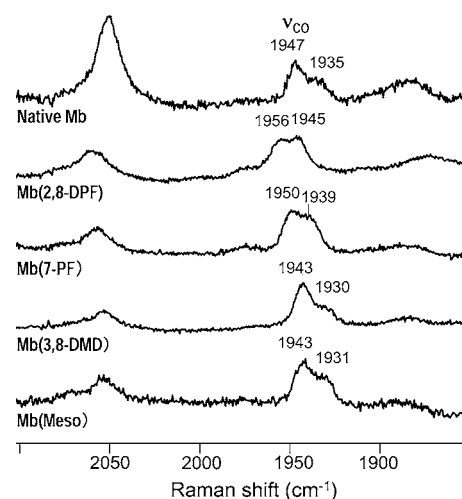


Figure 2. High-frequency regions of visible resonance Raman spectra of MbCO(Meso), MbCO(3,8-DMD), MbCO(7-PF), MbCO(2,8-DPF), and native MbCO at pH 7.40 and 25 °C. Positions of the individual component ν_{CO} bands of the proteins determined through fitting with Voigt profiles³⁶ (see Figures S3–S7, Supporting Information) are indicated with the spectra.

Fe–CO fragment.³⁵ Hence, the increase in number of ν_{CO} bands upon substitution of CF₃ group(s) (see Figure S5 and S6, Supporting Information) suggested that the number of conformational states taken by the Fe–CO fragment increases with decreasing ρ_{Fe} value, possibly due to weakening of the Fe–CO bond. The positions of the individual component ν_{CO} bands of the proteins were determined through fitting with Voigt profiles, which are convolutions of Gaussian and Lorentzian functions (see Figures S3–S7, Supporting Information),³⁶ and the high- and low-frequency ν_{CO} values ($\nu_{\text{CO(H)}}$ and $\nu_{\text{CO(L)}}$ values, respectively) and the weighted-average by the intensity of each band ($\nu_{\text{CO(ave)}}$) were determined (Table 2). As shown in Figure 2, the ν_{CO} bands of native MbCO

Table 2. Vibrational Frequencies of the Fe-Bound CO of Mb(CO)s at pH 7.40 and 25 °C; *pK*_a values of metMbs at 25 °C

Mb	ν_{CO}^a (cm ⁻¹)			ν_{FeC}^b (cm ⁻¹)	δ_{FeCO}^c (cm ⁻¹)	<i>pK</i> _a
	$\nu_{\text{CO(H)}}^d$	$\nu_{\text{CO(L)}}^e$	$\nu_{\text{CO(ave)}}^f$			
Mb(Meso)	1943	1931	1939	515	576	9.43 ^g
Mb(3,8-DMD)	1943	1930	1940	514	576	9.1 ^h
Native Mb	1947	1935	1943	512	576	8.90 ^g
Mb(7-PF)	1950	1939	1945	514	575	8.57 ^g
Mb(2,8-DPF)	1956	1945	1951	512	574	7.41 ^g

^aStretching frequency of Fe-bound CO. ^bFe–C stretching frequency. ^cFe–C–O bending frequency. ^d ν_{CO} value of the high-frequency band (see Figures S4–S8, Supporting Information). ^e ν_{CO} value of the low-frequency band (see Figures S4–S8, Supporting Information). ^fWeighted-average ν_{CO} value (see Figures S4–S8, Supporting Information). ^gObtained from ref 7. ^hObtained from ref 24.

appeared at 1947 cm⁻¹ with a shoulder at 1935 cm⁻¹ (Figure 2), and the determined values were larger by 2–3 cm⁻¹ than those previously reported, that is, a main band at 1944 cm⁻¹ with a shoulder near 1933 cm⁻¹.³⁷ Since the ν_{CO} bands were considerably broad (see Figures S3–S7, Supporting Information), uncertainty of 2–3 cm⁻¹ would be associated, as a

method-dependent variation, with determination of the positions of the individual component bands. The ν_{FeC} band of the protein also appeared as unresolved multiple peaks, possibly due to the multiple conformational states of the Fe–CO fragment, as in the case of the ν_{CO} band, and hence, accurate determination of their positions was quite difficult. CO isotope substitution measurements were made to estimate the frequencies of the ν_{FeC} bands of the proteins (see Figure S8, Supporting Information). Finally, in contrast to the ν_{CO} and ν_{FeC} bands, the δ_{FeCO} one was observed as a single component, although the band overlapped with other unassigned porphyrin ones. Hence, the position of the δ_{FeCO} band was determined through fitting with Voigt profiles³⁶ (see Figures S9–S13, Supporting Information).

As shown in Table 2, the ν_{CO} , ν_{FeC} , and δ_{FeCO} values were all affected by the heme modifications. In particular, the ν_{CO} value increased dramatically with CF_3 substitutions (Table 2). This finding is consistent with those of Tsubaki et al.,³⁷ who demonstrated that the ν_{CO} value increased upon replacement of the heme vinyl group(s) with electron-withdrawing formyl one(s). Comparison of the $\nu_{\text{CO(H)}}$ values of the proteins yielded a difference of 7 cm^{-1} for the Mb(Meso)/Mb(7-PF) system, which is one-half the value, 13 cm^{-1} , for the Mb(3,8-DMD)/Mb(2,8-DPF) one. Similarly, comparison of the $\nu_{\text{CO(L)}}$ values yielded a difference of 8 cm^{-1} for the Mb(Meso)/Mb(7-PF) system, which is also one-half the value, 15 cm^{-1} , for the Mb(3,8-DMD)/Mb(2,8-DPF) one. These results demonstrated the additive effect of the heme π -system perturbation on the ν_{CO} value, as reported for the formyl substitution system.³⁷ Furthermore, comparison of the ν_{FeC} bands of the proteins yielded a difference of 1 cm^{-1} for the Mb(Meso)/Mb(7-PF) system, which is one-half the value, 2 cm^{-1} , for the Mb(3,8-DMD)/Mb(2,8-DPF) one, which also demonstrated the additive effect of the heme π -system perturbation on the ν_{FeC} value, although the effect was rather small.

Finally, the low-frequency shift of the δ_{FeCO} value with increasing number of CF_3 substitutions suggested that the orientation of the Fe-bound CO, with respect to the heme in a protein is affected by the ρ_{Fe} value.

DISCUSSION

Functional Consequences of Heme Modifications.

We previously found that the O_2 affinity of Mb is regulated by the ρ_{Fe} value in such a manner that the O_2 affinity of a protein decreases, due to an increase in the $k_{\text{off}}(\text{O}_2)$ value, with a decrease in the ρ_{Fe} value.⁷ The O_2 binding parameters determined for Mb(2,8-DPF) indicated that, upon substitution of two CF_3 groups into 3,8-DMD, the $k_{\text{off}}(\text{O}_2)$ value increases by a factor of ~ 10 while the $k_{\text{on}}(\text{O}_2)$ one remains essentially unaltered (Table 1), and hence, these results were fully consistent with our previous findings. In the case of CO binding, the $k_{\text{on}}(\text{CO})$ and $k_{\text{off}}(\text{CO})$ values as well as the CO affinity increased on substitution of two CF_3 groups. These results were consistent with those of Sono et al.,³⁸ who demonstrated that substitution(s) of electron-withdrawing formyl group(s) in heme side chain(s) results in increasing $k_{\text{on}}(\text{CO})$ and $k_{\text{off}}(\text{CO})$ values and CO affinity. In contrast, comparison of the CO binding parameters between Mb(Meso) and Mb(7-PF) indicated that, upon substitution of one CF_3 group, the $k_{\text{on}}(\text{CO})$ and $k_{\text{off}}(\text{CO})$ values as well as the CO affinity remained nearly unaltered. The apparent discrepancy in the effects of substitution of CF_3 group(s) on the CO binding properties between the Mb(Meso)/Mb(7-PF) and the Mb(3,8-

DMD)/Mb(2,8-DPF) systems would be due to the presence of a significant heme orientational disorder³³ in Mb(7-PF). Mb(7-PF) at equilibrium exhibits a M form: m form ($M:m$ (see Figure S14, Supporting Information)) ratio of $\sim 1.0:2.2$.³⁹ The $M:m$ ratio is $\sim 9:1$ in Mb(Meso),³⁹ and there is no heme orientational disorder in Mb(3,8-DMD) and Mb(2,8-DPF). Studies on Mb(7-PF) with a series of $M:m$ ratios, with highly precise measurements, are needed for detailed elucidation of the effects of the heme orientational disorder on the CO binding properties of the protein, because the CO binding of Mb(7-PF) could be analyzed using single-exponential kinetics (see Figure S15, Supporting Information), and the ligand binding properties of Mb have been shown to be almost independent of the heme orientation with respect to the protein moiety.⁴⁰

Correlation between the Vibrational Frequencies and Electron Density of the Heme Fe Atom. As described above, we observed additive effects of the heme π -system perturbation on the ν_{CO} and ν_{FeC} values. As shown in Table 2, similar additively was also observed between the pK_a value and the number of CF_3 substitutions, that is, the pK_a difference of 0.86 for the Mb(Meso)/Mb(7-PF) system is one-half the value, 1.70, for the Mb(3,8-DMD)/Mb(2,8-DPF) one. In fact, plots of the $\nu_{\text{CO(H)}}$ values of the proteins against the pK_a ones can be described by a linear function expressed as $\nu_{\text{CO(H)}/\text{cm}^{-1}} = -6.818 \times \text{pK}_a + 2007$, with correlation coefficient (r) = -0.9716 , and the relationship between the $\nu_{\text{CO(L)}}$ and the pK_a values can be also represented by $\nu_{\text{CO(L)}/\text{cm}^{-1}} = -7.565 \times \text{pK}_a + 2002$, with $r = -0.9531$ (Figure 3). Similarly, the $\nu_{\text{CO(ave)}}$

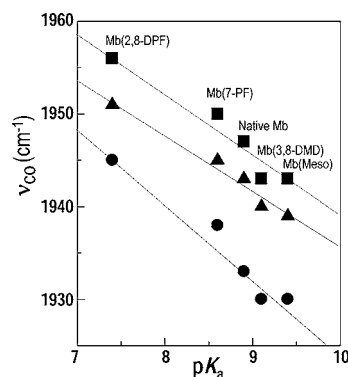


Figure 3. Plots of the high-frequency ν_{CO} ($\nu_{\text{CO(H)}}$ (■)), low-frequency ν_{CO} ($\nu_{\text{CO(L)}}$ (●)), and weighted-average ν_{CO} ($\nu_{\text{CO(ave)}}$ (▲)) values of MbCOs against the pK_a ones of the acid–alkaline transition in metMbs. Plots can be represented by straight lines.

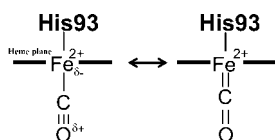
value exhibited a linear relationship with the pK_a value, that is, $\nu_{\text{CO(ave)}/\text{cm}^{-1}} = -6.071 \times \text{pK}_a + 1996$, with $r = -0.9874$ (Figure 3). These results not only demonstrated that the ν_{CO} value is affected by the ρ_{Fe} value, as the pK_a value is, but also confirmed that the effects of the heme modifications on the ρ_{Fe} value are essentially independent of the oxidation state of the heme Fe atom.

Neya et al.⁴¹ demonstrated, on X-ray structural determination, that the overall protein structure and side chain conformations of Mb reconstituted with porphine are essentially identical to those of the native protein. Furthermore, they also revealed that the protein structure properties of the globin fold together with the structure of the heme active site are inherent in its amino acid sequence and are not largely affected by the acquired heme–protein interaction.⁴² In fact, as

in the case of the ^1H NMR spectrum of the met-cyano form of native Mb, the C_γH and $\text{C}_\delta\text{H}_3$ proton signals of Ile99 in all reconstituted Mbs were resolved in ~ -4 to ~ -10 ppm, confirming that the orientations of the hemes with respect to the polypeptide chains in these reconstituted proteins are similar to that in the native one (see Figure S16, Supporting Information).

Hence, the differences in the vibrational frequencies among the proteins can be attributed primarily to the electronic effects exerted by the heme modifications. The relationship between the ν_{CO} and the $\text{p}K_a$ (and hence ρ_{Fe}) values could be interpreted in terms of the resonance between the two canonical forms of the Fe–CO fragment, represented by the valence bond formalism (Scheme 1).²⁶ The larger the ρ_{Fe} value,

Scheme 1. Resonance between the Two Canonical Forms of the Fe–CO Fragment, Represented by the Valence Bond Formalism^{26a}



^aThe larger the ρ_{Fe} value, the better the heme Fe atom can serve as a π donor to CO. The stronger the Fe–CO bond, the larger will be the bond order of the Fe–CO bond, the smaller will be the C–O bond order, and hence the weaker will be the C–O bond.

the better the heme Fe atom can serve as a π donor to CO. The stronger the Fe–CO bond, the larger will be the bond order of the Fe–CO bond, the smaller will be the C–O bond order, and hence the weaker will be the C–O bond. Consequently, the strength of the Fe–CO and C–O bonds decreases and increases, respectively, with decreasing ρ_{Fe} value. As a result, a reciprocal relationship holds between the ν_{FeC} and the ν_{CO} values, as demonstrated previously.⁴³ A similar $\nu_{\text{FeC}}-\nu_{\text{CO}}$ reciprocal relationship was observed for the proteins considered in the study. This finding indicated that the π back-donation of the heme Fe atom to CO (Fe \rightarrow CO π back-donation) is affected by the in-plane electronic perturbation of the heme π system induced through the heme modifications.

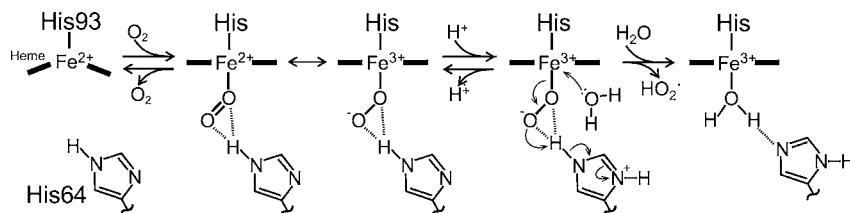
The variation of the estimated ν_{FeC} values among the proteins was small, that is, the slopes of the plots of the ν_{FeC} values against the $\nu_{\text{CO(H)}}$, ν_{CO} , and $\nu_{\text{CO(ave)}}$ ones for the proteins were smaller by factors from $\sim 1/4$ to $\sim 1/5$ relative to the value determined through studies of a variety of heme derivatives and hemoproteins possessing diverse axial ligands.⁴³ The bonding of CO to the heme Fe atom is thought to involve a synergic

process with donation of the lone pair electrons of the C atom into an empty d_σ (d_z^2) orbital of the metal (Fe \leftarrow CO σ donation), together with the Fe \rightarrow CO π back-donation. In contrast to the case of the Fe \rightarrow CO π back-donation, the Fe \leftarrow CO σ donation is expected to increase with decreasing ρ_{Fe} value. Consequently, the small effects of the heme modifications on the ν_{FeC} value might be attributed to a result of a countervailing relationship between the effects of a change in the ρ_{Fe} value on the Fe \leftarrow CO σ donation and Fe \rightarrow CO π back-donation.

Electronic Mechanisms for O₂/CO Discrimination and Autoxidation of Mb.

Elucidation of molecular mechanisms responsible for discrimination of exogenous ligands by hemoproteins has been one of the central issues in not only bioinorganic chemistry but also biological science. Particularly, the mechanism of the discrimination between O₂ and CO by Mb has been investigated exhaustively for a long time.^{4,5,34,44} Some mechanisms have been proposed to account for the ability of the protein to stabilize Fe-bound O₂ and discriminate against CO binding. It is well documented that coordination of O₂ to heme Fe atom is stabilized by a factor of ~ 1000 by formation of a hydrogen bond between the Fe-bound O₂ and His64, whereas the CO affinity of the protein is only slightly affected by interaction between the Fe-bound CO and His64.⁵ Furthermore, a steric mechanism involving concerted motions of the heme, the heme Fe atom, and helices E and F has been also proposed to selectively inhibit the CO binding to the protein.⁴⁴ In addition to these two mechanisms, our study revealed that preferential binding of CO to the protein over O₂ is enhanced with decreasing ρ_{Fe} value, as can be seen from the M values of the proteins (Table 1).⁷ Electronic control of the M value is achieved through the effect of a change in the ρ_{Fe} value on the O₂ affinity, which can be interpreted in terms of the resonance process between the Fe²⁺–O₂ and Fe³⁺–O₂[–]-like species⁴⁵ (Scheme 2). A decrease in the ρ_{Fe} value is expected to hinder formation of the Fe³⁺–O₂[–]-like species through obstruction of Fe–O bond polarization, resulting in a shift of the resonance toward the Fe²⁺–O₂ species. Since O₂ dissociation from the heme Fe atom is thought to occur only at the Fe²⁺–O₂ bond, stabilization of the Fe²⁺–O₂ bond over the Fe³⁺–O₂[–]-like one with decreasing ρ_{Fe} value should result in an increase in the O₂ dissociation rate,⁷ which lowers the O₂ affinity. On the other hand, in the case of the Fe-bound CO, although the resonance between the two canonical forms of the Fe–CO fragment (scheme 1) is affected by the ρ_{Fe} value, the effect of a change in the ρ_{Fe} value on the CO affinity was rather small, as demonstrated in this study.

Scheme 2. Oxygenation of Mb and Reaction Mechanism for Autoxidation Proposed by Shikama^{46,47a}



^aThe binding of O₂ to the heme Fe²⁺ is stabilized by the hydrogen bonding between the Fe-bound O₂ and His64,⁴⁴ and the third drawing is only a proposed structure.^{3,45} Dissociation of hydroperoxyl radical HO₂[•] from the heme Fe³⁺, followed by instantaneous coordination of H₂O to heme Fe³⁺, the fourth drawing, is only a speculative process, and simultaneous accommodation of both H₂O and Fe-bound O₂ hydrogen bonded to His64 in the heme pocket of the protein would be possible.

Furthermore, as demonstrated previously,⁸ the ρ_{Fe} value is also a determinant for the rate of the autoxidation (k_{ox}), which is spontaneous conversion of the $\text{Fe}^{2+}-\text{O}_2$ species to the $\text{Fe}^{3+}-\text{H}_2\text{O}$ one (scheme 2). According to the reaction mechanism proposed by Shikama,^{46,47} the acid-catalysis process occurs through protonation of Fe^{2+} -bound O_2 , which leads to dissociation of hydroperoxyl radical HO_2^\bullet from the active site of the protein followed by ionization of HO_2^\bullet into H^+ and superoxide anion radical $\text{O}_2^{\bullet-}$. Therefore, since the H^+ affinity of the Fe^{2+} -bound O_2 is lower than that of the $\text{Fe}^{3+}-\text{O}_2^-$ -like species, stabilization of the former over the latter with decreasing the ρ_{Fe} value should inhibit the acid-catalysis process for autoxidation of the protein, resulting in a decreased k_{ox} value (Table 1).⁸

CONCLUSION

We demonstrated that the ν_{CO} value of Mb correlates well with the $\text{p}K_{\text{a}}$ value in such a manner that a protein possessing a lower $\text{p}K_{\text{a}}$ value exhibits a higher ν_{CO} one. The $\nu_{\text{CO}}-\text{p}K_{\text{a}}$ correlation could be interpreted simply in terms of the resonance between the two canonical forms of the $\text{Fe}-\text{CO}$ fragment, represented by the valence bond formalism. Furthermore, the linear correlation indicated not only that the effects of the heme modifications on the ρ_{Fe} value are independent of the oxidation state of the heme Fe atom but also that the ν_{CO} value can be used as a sensitive measure of the ρ_{Fe} value in a protein in order to gain a deeper understanding of the molecular mechanism responsible for electronic regulation of the heme Fe reactivity.

ASSOCIATED CONTENT

Supporting Information

Figures S1–S16. This material is available free of charge via the Internet at <http://pubs.acs.org>.

AUTHOR INFORMATION

Corresponding Author

*Phone/Fax: +81 29 853 6521 (Y.Y.); +81 791 58 0182 (T.O.). E-mail: yamamoto@chem.tsukuba.ac.jp (Y.Y.); ogura@sci.u-hyogo.ac.jp (T.O.).

Notes

The authors declare no competing financial interest.

ACKNOWLEDGMENTS

This work was supported by a Grant-in-Aid for Scientific Research on Innovative Areas (nos. 23108703, “ π -Space”) from the Ministry of Education, Culture, Sports, Science and Technology, Japan, the Yazaki Memorial Foundation for Science and Technology, and the NOVARTIS Foundation (Japan) for the Promotion of Science.

REFERENCES

- (1) Chu, K.; Vojtchovsky, J.; McMahon, B. H.; Sweet, R. M.; Berendzen, J.; Schlichting, I. *Nature* **2000**, *403*, 921–923.
- (2) Schotte, F.; Lim, M.; Jackson, T. A.; Smirnov, A. V.; Soman, J.; Olson, J. S.; Phillips, G. N., Jr.; Wulff, M.; Anfirud, P. A. *Science* **2003**, *300*, 1944–1947.
- (3) Antonini, E.; Brunori, M. In *Hemoglobins and Myoglobins and their Reactions with Ligands*; North Holland Publishing: Amsterdam, 1971.
- (4) Springer, B. A.; Sligar, S. G.; Olson, J. S.; Phillips, G. N., Jr. *Chem. Rev.* **1994**, *94*, 699–714.
- (5) Olson, J. S.; Phillips, G. N., Jr. *J. Biol. Inorg. Chem.* **1997**, *2*, 544–552.

- (6) Capece, L.; Marti, M. A.; Crespo, A.; Doctorovich, F.; Estrin, D. A. *J. Am. Chem. Soc.* **2006**, *128*, 12455–12461.
- (7) Shibata, T.; Nagao, S.; Fukaya, M.; Tai, H.; Nagatomo, S.; Morihashi, K.; Matsuo, T.; Hirota, S.; Suzuki, A.; Imai, K.; Yamamoto, Y. *J. Am. Chem. Soc.* **2010**, *132*, 6091–6098.
- (8) Shibata, T.; Matsumoto, D.; Nishimura, R.; Tai, H.; Matsuoka, A.; Nagao, S.; Matsuo, T.; Hirota, S.; Imai, K.; Neya, S.; Suzuki, A.; Yamamoto, Y. *Inorg. Chem.* **2012**, *51*, 11955–11960.
- (9) Giacometti, G. M.; Da Ros, A.; Antonini, E.; Brunori, M. *Biochemistry* **1975**, *14*, 1584–1588.
- (10) Iizuka, T.; Morishima, I. *Biochim. Biophys. Acta* **1975**, *400*, 143–153.
- (11) McGrath, T. M.; La Mar, G. N. *Biochim. Biophys. Acta* **1978**, *534*, 99–111.
- (12) Pande, U.; La Mar, G. N.; Lecomte, J. T. L.; Ascoli, F.; Brunori, M.; Smith, K. M.; Pandey, R. K.; Parish, D. W.; Thanabal, V. *Biochemistry* **1986**, *25*, 5638–5646.
- (13) Rossi-Fanelli, A.; Antonini, E. *Biochimica* **1957**, *22*, 336–344.
- (14) Seamounts, B.; Forster, R. E.; George, P. *J. Biol. Chem.* **1971**, *246*, 5391–5397.
- (15) Suzuki, T. *Biochim. Biophys. Acta* **1987**, *914*, 170–176.
- (16) Yamamoto, Y.; Ossawa, A.; Inoue, Y.; Chujo, R.; Suzuki, T. *Eur. J. Biochem.* **1990**, *192*, 225–229.
- (17) Yamamoto, Y.; Suzuki, T.; Hori, H. *Biochim. Biophys. Acta* **1993**, *1203*, 267–275.
- (18) Koshikawa, K.; Yamamoto, Y.; Kamimura, S.; Matsuoka, A.; Shikama, K. *Biochim. Biophys. Acta* **1998**, *1385*, 89–100.
- (19) Yamamoto, Y.; Kurihara, N.; Egawa, T.; Shimada, H.; Ishimura, Y. *Biochim. Biophys. Acta* **1999**, *1433*, 27–44.
- (20) Makinen, M. W.; Houtchens, R. A.; Caughey, W. S. *Proc. Natl. Acad. Sci. U.S.A.* **1979**, *76*, 6042–6046.
- (21) Shimada, H.; Caughey, W. S. *J. Biol. Chem.* **1982**, *257*, 11893–11900.
- (22) Kerr, E. A.; Yu, N. T. In *Biological Applications of Raman Spectroscopy*; Spiro, T. G., Ed.; Wiley-Interscience: New York, 1988; Vol. 111, Chapter 2.
- (23) Chang, C. K.; Ward, B.; Ebina, S. *Arch. Biochem. Biophys.* **1984**, *231*, 366–371.
- (24) Neya, S.; Suzuki, M.; Hoshino, T.; Ode, H.; Imai, K.; Komatsu, T.; Ikezaki, A.; Nakamura, M.; Furutani, Y.; Kandori, H. *Biochemistry* **2010**, *49*, 5642–5650.
- (25) Toi, H.; Homma, M.; Suzuki, A.; Ogoshi, H. *J. Chem. Soc., Chem. Commun.* **1985**, 1791–1792.
- (26) Alben, J. O.; Caughey, W. S. *Biochemistry* **1968**, *7*, 175–183.
- (27) Teale, F. W. J. *Biochim. Biophys. Acta* **1959**, *35*, 543.
- (28) Matsuo, T.; Dejima, H.; Hirota, S.; Murata, D.; Sato, H.; Ikegami, T.; Hori, H.; Hisaeda, Y.; Hayashi, T. *J. Am. Chem. Soc.* **2004**, *126*, 16007–16017.
- (29) Hayashi, T.; Dejima, H.; Matsuo, T.; Sato, H.; Murata, D.; Hisaeda, Y. *J. Am. Chem. Soc.* **2002**, *124*, 11226–11227.
- (30) Rohlfs, R. J.; Mathews, A. J.; Carver, T. E.; Olson, J. S.; Springer, B. A.; Egeberg, K. D.; Sligar, S. G. *J. Biol. Chem.* **1990**, *265*, 3168–3176.
- (31) Matsuo, T.; Ikegami, T.; Sato, H.; Hisaeda, Y.; Hayashi, T. *J. Inorg. Biochem.* **2006**, *100*, 1265–1271.
- (32) Kitanishi, K.; Kobayashi, K.; Kawamura, Y.; Ishigami, I.; Ogura, T.; Nakajima, K.; Igarashi, J.; Tanaka, A.; Shimizu, T. *Biochemistry* **2010**, *49*, 10381–10393.
- (33) La Mar, G. N.; Budd, D. L.; Viscio, D. B.; Smith, K. M.; Langry, L. C. *Proc. Natl. Acad. Sci. U.S.A.* **1978**, *75*, 5755–5759.
- (34) Springer, B. A.; Egeberg, K. D.; Sligar, S. G.; Rohlfs, R. J.; Mathews, A. J.; Olson, J. S. *J. Biol. Chem.* **1989**, *264*, 3057–3060.
- (35) Caughey, W. S.; Shimada, H.; Choc, M. G.; Tucker, M. P. *Proc. Natl. Acad. Sci. U.S.A.* **1981**, *78*, 2903–2907.
- (36) Anderson, C. L.; Hester, R. E.; Moore, J. N. *Biochim. Biophys. Acta* **1997**, *1338*, 107–120.
- (37) Tsubaki, M.; Srivastava, R. B.; Yu, N. T. *Biochemistry* **1982**, *21*, 1132–1140.

- (38) Sono, M.; Smith, P. D.; McCray, J. A.; Asakura, T. *J. Biol. Chem.* **1976**, *251*, 1418–1426.
- (39) Yamamoto, Y.; Nagao, S.; Hirai, Y.; Inose, T.; Terui, N.; Mita, H.; Suzuki, A. *J. Biol. Inorg. Chem.* **2004**, *9*, 152–160.
- (40) Light, W. R.; Rohlf, R. J.; Palmer, G.; Olson, J. S. *J. Biol. Chem.* **1987**, *262*, 46–52.
- (41) Neya, S.; Funasaki, N.; Sato, T.; Igarashi, N.; Tanaka, N. *J. Biol. Chem.* **1993**, *268*, 8935–8942.
- (42) Neya, S.; Funasaki, N.; Shiro, Y.; Iizuka, T.; Imai, K. *Biochim. Biophys. Acta* **1994**, *1208*, 31–37.
- (43) Li, X. -Y.; Spiro, T. G. *J. Am. Chem. Soc.* **1988**, *110*, 6024–6033.
- (44) Kachalova, G. S.; Popov, A. N.; Bartunik, H. D. *Science* **1999**, *284*, 473–476.
- (45) Maxwell, J. C.; Volpe, J. A.; Barlow, C. H.; Caughey, W. S. *Biochem. Biophys. Res. Commun.* **1974**, *58*, 166–171.
- (46) Shikama, K. *Coord. Chem. Rev.* **1988**, *83*, 73–91.
- (47) Shikama, K. *Prog. Biophys. Mol. Biol.* **2006**, *91*, 83–162.